

# Filaggrin Peptides with $\beta$ -Hairpin Structure Bind Rheumatoid Arthritis Antibodies\*\*

Sabrina Fischer and Armin Geyer\*

**Abstract:** In the early detection of rheumatoid arthritis (RA) synthetic filaggrin peptides serve as antigens for rheumatoid-specific autoantibodies (anti-citrullinated peptide antibody, ACPA) in ELISA tests. In this work we present a peptide that exhibits the binding epitope of ACPA in the form of a stable folding  $\beta$ -hairpin. The homogeneity of the peptide folding was confirmed by NMR spectroscopy and might lead to the first proposed structure of the antibody-bound conformation of the epitope.

Citrullinated peptides are used in the diagnosis of rheumatoid arthritis (RA), because they bind selectively a group of autoantibodies (anti-citrullinated peptide antibody, ACPA) formed in the early stage of RA. Van Venrooij et al. showed that the section 303–324 of the human filaggrin sequence is suitable for antibody detection, wherein the noncanonical amino acid citrulline was found to be essential.<sup>[1,2]</sup> One result of their work was a cyclic disulfide derivative of this peptide sequence, which exhibits an improved binding to ACPA and is used in the commercially available CCP ELISA test for early diagnosis of RA.<sup>[3]</sup> This peptide, cfc1-cyc 1, is shown in Figure 1. The specificity of this assay is 89–98 %, while the sensitivity is reported in different studies to be between 41 % and 87 % for an established RA.<sup>[3–6]</sup> Meanwhile two further generations of the CCP ELISA tests have been developed with different citrullinated peptides as targets, which increase the sensitivity of the tests.<sup>[7–9]</sup> It is evident that the essential hapten for the binding of the antibody is the urea group present in citrulline, because mutants with the isosteric amino acid arginine are not detected.<sup>[1,2,10]</sup> Since cfc1-cyc 1 does not have a preferred conformation, the geometry of the binding epitope is still speculative (vide infra). If the disulfide macrocyclization already leads to an improved binding of the antibody, additional structural restriction of the epitope and the impact on selectivity and affinity has to be investigated.

Peptide ligands are recognized as  $\beta$ -turns by proteins, and this type of binding is expected for antibody-binding peptides, too.<sup>[11–13]</sup> Obviously, the epitope of an antibody-binding

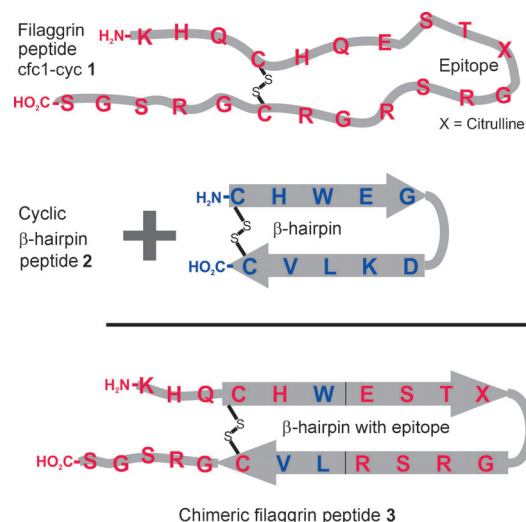


**Figure 1.** Concept for the synthesis of chimeric filaggrin peptides by combination of the antibody-binding epitope in cfc1-cyc 1 with the stabilizing properties of the cyclic  $\beta$ -hairpin 2. The chimeric filaggrin peptide 3 is obtained by mutation of only three amino acids in cfc1-cyc 1.

peptide should be presented in a  $\beta$ -turn within a conformationally stable  $\beta$ -hairpin. There are different well-known strategies to direct peptides into conformationally homogeneous structures. D amino acids are used to stabilize a  $\beta$ -turn.<sup>[14]</sup> The concept of linking the structure and biological activity of peptides was already shown by Kessler et al. with integrin-binding RGD pentapeptides.<sup>[15,16]</sup> A D-Pro-L-Pro motif was used as a turn mimetic to give biologically active peptides a defined conformation.<sup>[17]</sup> Numerous dipeptide mimetics are known for  $\beta$ -hairpins, forming a  $\beta$ -turn and inducing or stabilizing the hairpin fold, such as Hot = Tap, which even can mediate a protein–protein interaction.<sup>[18]</sup>

In this work we describe the transfer of stabilizing interactions in a model hairpin structural motif to a biologically active filaggrin sequence. The conformationally uniform  $\beta$ -hairpin Bhp HV (2) published by Cochran et al. was used as a model hairpin peptide. This 10-mer cyclic hairpin peptide 2 is characterized by the large signal dispersion of the chemical shifts in the <sup>1</sup>H NMR spectrum, hydrogen bonds, and distinct side-chain rotamers.<sup>[19]</sup> In contrast, the <sup>1</sup>H NMR spectrum of the filaggrin peptide 1 shows fast conformational averaging characterized by the low dispersion of chemical shifts and averaged coupling constants. The sequence similarity between these two peptides is noticeable since the stabilizing structural motif of model peptide 2 consisting of six amino acids is integrated in the filaggrin peptide 1 by only three mutations. The preferred binding motif of ACPA could be

[\*] S. Fischer, Prof. A. Geyer  
Faculty of Chemistry, Philipps University Marburg  
Hans-Meerwein-Strasse, 35032 Marburg (Germany)  
E-mail: geyer@staff.uni-marburg.de

[\*\*] We thank Dr. Y. Röttger and Dr. M. Gold (in the research group of Prof. R. Dodel, Neurological Clinic, Philipps University Marburg) for support in the preparation of Dot Blot and ELISA experiments and D. Brödjé (University Medical Center, Marburg) for human ACPA.

Supporting information for this article is available on the WWW under <http://dx.doi.org/10.1002/anie.201309873>.

elucidated by determining the binding affinity of these conformationally homogeneous peptides. This work focuses on modified filaggrin peptides, which are suitable for the investigation of antibody–peptide interactions.

In the  $\beta$ -hairpin peptide **2** developed by Cochran (sequence in Figure 1), hydrophobic interactions exist between the side chains of His<sup>2</sup> and Trp<sup>3</sup> and the side chains of Leu<sup>8</sup> and Val<sup>9</sup> on the opposite side. The stabilizing effect of the Trp<sup>3</sup>–Leu<sup>8</sup> pair to the  $\beta$ -hairpin structure of **2** has already been shown in substitution studies.<sup>[20]</sup> In addition, the interaction between Val<sup>9</sup> and the disulfide bridge causes local stabilization of the peptide backbone twist.<sup>[19]</sup> These three hydrophobic or aromatic amino acids of the N- and C-terminus are followed by Glu<sup>4</sup> and Lys<sup>7</sup> on the opposite side. Glu<sup>7</sup> and Arg<sup>14</sup> of **1** are in a similar relative arrangement (Figure 1). The hydrophobic cluster is completed by the three mutations Gln<sup>6</sup>→Trp, Gly<sup>15</sup>→Leu, and Arg<sup>16</sup>→Val, thus transferring the stabilizing effects of the hairpin **2** to the filaggrin sequence.

The structural characterization of the chimeric filaggrin peptides was performed with cyclic peptides, which were shortened by the unstructured amino acids outside of the macrocyclic ring. The cyclic 14-mer CHWESTXGRSRLVC (**4**, X = citrulline) was dissolved in aqueous phosphate buffer (50 mM, pH 7.0) to allow a native fold. The large signal dispersion in the <sup>1</sup>H NMR spectrum is the most evident difference between the folded peptide **4** and the nonstructured **1**. The methyl groups at about 1 ppm are strongly shielded by the aromatic amino acids and shifted upfield to about –0.3 ppm. The amide NH signals double the range of chemical shifts to approximately 1.5 ppm (Figure 2). This effect is only observed after the oxidation to the disulfide because the disulfide bond is essential for the folding.

To determine whether the structure is stabilized by one of these three mutations, or by the combination of the three amino acids Trp, Leu, and Val, the peptides **5**, **6**, and **7** (Table 1) were synthesized, each with a single back mutation. Together, the dispersion of the amide protons and the shielding of Leu<sup>8</sup>Me show that each of the three has a significant influence on the folding. The back mutation of Val<sup>16</sup> to Arg in peptide **5** has the least influence on the peptide conformation, while the absence of Leu<sup>15</sup> in peptide **7** results in a small dispersion in the <sup>1</sup>H NMR spectrum (Table 1, Figure 2). The back mutation of Trp<sup>6</sup> to Gln in peptide **6**, however, allows residual folding. In conclusion, the peptide

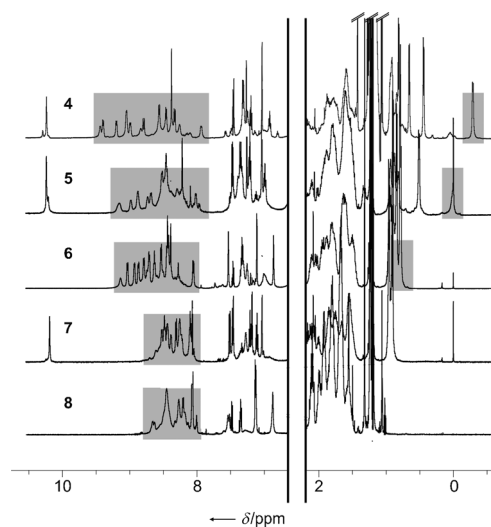


**Figure 2.** <sup>1</sup>H NMR spectra of peptides **4–8** (600 MHz, 280 K, phosphate buffer (50 mM, pH 7)/D<sub>2</sub>O 9:1). The upfield and downfield areas of the spectra display the decrease of the signal dispersion on going from **4** to **8**. The stability of the hairpins (each marked in gray) was defined by the signal dispersion in the amide range and the upfield shift of the Leu<sup>8</sup>Me. Peptide **4** shows the largest dispersion, while no preferred conformation is observed for **7** and **8**. The complete spectra are shown in the Supporting Information.

conformation is based mainly on the disulfide bridge and hydrophobic interaction between Trp<sup>6</sup> and Leu<sup>15</sup>.

The  $\beta$ I'/ $\beta$ II'-flip of the  $\beta$ -turn in the rigid hairpin of **4** leads to exchange broadening of the amide protons of Gly<sup>11</sup> and Cit<sup>10</sup>. With either the amino acids Ala (peptide **9**) or D-Ala (peptide **10**) at the position of Gly<sup>11</sup>, one  $\beta$ -turn structure is energetically favored, wherein D-Ala forms a  $\beta$ II'-turn.<sup>[18]</sup> While the D-Ala peptide has the same dispersion in the <sup>1</sup>H NMR spectrum as **4**, the mutation to Ala at this position leads to a significantly lower dispersion. In contrast to the D-Ala mutant, the amide proton signal of Gly at the *i*+2 position is strongly broadened in peptide **4**. It is assumed that no consistent turn structure is formed in peptide **4**, but rather a rapid conformational change between  $\beta$ I' and  $\beta$ II'-turn takes place.

Signal dispersion alone, however, does not suffice for conformational analysis. The progression of hydrogen bonds is characteristic for a  $\beta$ -hairpin. They are formed between every second opposing pair of amino acids, causing an alternating sequence of internally and externally oriented amide protons within the peptide sequence. As a consequence, different temperature dependences are observed for the amide proton chemical shifts in the <sup>1</sup>H NMR (Figure 3). The amide protons of hydrogen-bonded amino acids show a small temperature gradient (3.3 to 9.0 ppb K<sup>–1</sup>), whereas the signals of the non-hydrogen-bonded amino acids have a large temperature gradient (9.2 to 14.6 ppb K<sup>–1</sup>, Figure 3). This alternating series of small and large temperature dependences is a general characteristic of  $\beta$ -hairpin structures.

Detailed geometric parameters of the  $\beta$ -hairpin structure of **4** were obtained from the NOE contacts in the NOESY spectrum (600 MHz, 280 K, mixing time 100 ms). NOE contacts are observed between the side-chain protons across

**Table 1:** Correlation of the amount of peptide folding with signal dispersion in the <sup>1</sup>H NMR.

Peptide <sup>[a]</sup>	$\delta(\text{Leu}^8\text{Me})$ [ppm] <sup>[b]</sup>	$\Delta\delta(\text{NH})$ [ppm] <sup>[c]</sup>
CHWESTXGRSRLVC ( <b>4</b> )	–0.28	1.60
CHWESTXGRSRL <b>R</b> C ( <b>5</b> )	0.02	1.24
CH <b>Q</b> ESTXGRSRLVC ( <b>6</b> )	0.79	1.15
CHWESTXGRSR <b>G</b> VC ( <b>7</b> )	— <sup>[e]</sup>	0.67
CH <b>Q</b> ESTXGRSR <b>G</b> RC ( <b>8</b> ) <sup>[d]</sup>	— <sup>[e]</sup>	0.70

[a] Sequences of cyclic disulfide peptides. Bold-face font denotes mutations relative to **4**. X = citrulline. [b] Chemical shift  $\delta$  of the upfield-shifted Leu methyl group. [c] Dispersion of the chemical shift  $\delta$  in the amide range. [d] Native filaggrin sequence. [e] No Leu in this sequence.

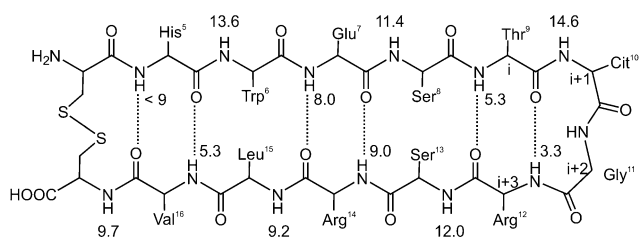


**Figure 3.** Illustration of the  $\beta$ -hairpin peptide **4**, wherein the temperature dependence of the chemical shift of the amide proton in  $^1\text{H}$  NMR spectrum (600 MHz, 280–310 K, phosphate buffer (50 mM, pH 7)/ $\text{D}_2\text{O}$  9:1) is given (in  $\text{ppb K}^{-1}$ ). The amide protons of the hydrogen-bonded amino acids have a lower temperature dependence in the  $^1\text{H}$  NMR spectrum.<sup>[21]</sup> The highest (14.6  $\text{ppb K}^{-1}$ ) and the lowest (3.3  $\text{ppb K}^{-1}$ ) values are observed for the amino acids in the turn. See the text for further details.

the two strands of the  $\beta$ -hairpin. There are only contacts within the hydrogen-bonded or nonbonded amino acids, which can be found in a  $\beta$ -sheet structure on the same side of the peptide backbone. This is schematically represented by a zigzag structure in which the hydrogen-bonded amino acids are located above the backbone while the nonbonded amino acids are below the backbone (Figure 4).

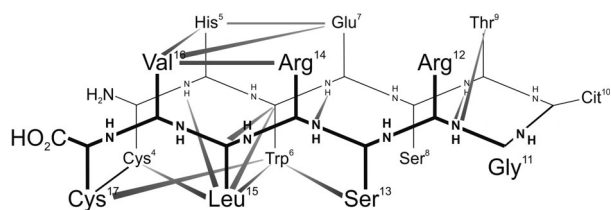


**Figure 4.** Schematic illustration of the structurally relevant NOE contacts in **4** (from NOESY spectrum, 600 MHz, 280 K, phosphate buffer (50 mM, pH 7)/ $\text{D}_2\text{O}$  9:1). The zigzag representation of the  $\beta$ -hairpin shows which amino acid residues face each other within the hairpin structure. All hydrogen-bonded amino acids are above the peptide backbone. NOE contacts between the hairpin strands are only visible when both amino acids are above or below the peptide backbone. For example, Leu<sup>15</sup> exhibits NOE contacts with almost all through-space neighbors below the hairpins. Most NOE contacts are observed within the Cochran hairpin motif.

The large number of characteristic NOE contacts between the N-terminal amino acids Cys, His, and Trp as well as the C-terminal amino acids Cys, Val, and Leu is noticeable. The stabilization of a cyclic  $\beta$ -hairpin structure by a Val/His pair adjacent to a disulfide has been described for  $\text{CX}_8\text{C}$  peptides.<sup>[19]</sup> In addition, hydrophobic interactions can take place between Val and His, as well as between Leu and Trp and cause a further stabilization of the structure. These six amino acids work like a clamp to rigidify the structure, directing the residual peptide chain into the  $\beta$ -turn geometry, even though this chain is longer than that in **2**.

In addition to the NOE contacts the identification of the dominating side-chain rotamer is an independent, geometrically meaningful parameter. This was done by the prochiral assignment of  $\beta$ -methylene groups. The side-chain rotamers of the individual amino acid residues were quantified as

further conformational information (Table 2). For this, the  $^3J$  couplings between  $\alpha$  and  $\beta$  protons were assigned from the  $^1\text{H}$  and 2D NMR spectra and the distances between the  $\alpha$  or amide proton and the  $\beta$  protons were determined from the

**Table 2:** Diastereotopic assignment of the  $\beta$  protons and determination of the predominant rotamer around the  $\chi_1$  angles for the amino acids in the  $\beta$ -hairpin **4**.

Amino acid <sup>[a]</sup>	$\beta\text{H}^{\text{h[b]}}$	$\beta\text{H}^{\text{t[c]}}$	$\chi_1$
Cys <sup>4</sup>	proS	proR	$-60^\circ$
His <sup>5</sup>	proR	proS	$+60^\circ$
Trp <sup>6</sup>	proR	proS	$-60^\circ$
Glu <sup>7</sup>	proR	proS	$-60^\circ$
Thr <sup>9</sup>			$-60^\circ$
Cit <sup>10</sup>	proS	proR	$180^\circ$
Arg <sup>12</sup>	proR	proS	$-60^\circ$
Leu <sup>15</sup>	proS	proR	$-60^\circ$
Val <sup>16</sup>			$180^\circ$
Cys <sup>17</sup>	proR	proS	$-60^\circ$

[a] Order of the amino acids corresponding to the sequence in **4**. For Ser<sup>8</sup>, Ser<sup>13</sup>, and Arg<sup>14</sup> no determination could be carried out, since higher order spin systems are present. [b]  $\beta$ -Proton of the amino acid with the upfield chemical shift  $\delta$ . [c]  $\beta$ -Proton of the amino acid with the downfield chemical shift  $\delta$ .

NOESY spectrum. The side-chain conformations were assigned based on the assumption that only three energetically favorable rotamers contribute to the conformational equilibrium ( $\chi_1 = -60^\circ, 180^\circ, 60^\circ$ ). The conformation of His<sup>5</sup> with the sterically unfavorable  $\chi_1$  angle of  $+60^\circ$  is remarkable but characteristic of the Cochran motif. The imidazole ring is oriented toward the isopropyl group of Val<sup>16</sup>, indicating the stabilizing interaction between the two side chains. Even the conformation about the  $\chi_2$  angle of His<sup>5</sup> was determined, because from the  $\delta 2$  proton of the imidazole ring only NOE contacts are visible with the side chain of Glu<sup>7</sup> and from the  $\epsilon 1$  proton with Val<sup>16</sup>. Along the same rationale, the indole ring of the Trp<sup>6</sup> and the Leu<sup>15</sup> side chain were aligned along one another.

A structural model was created and a molecular dynamics simulation with HyperChem<sup>[22]</sup> was performed based on the NMR spectroscopic data. The energy-minimized structure is shown in Figure 5.

The obtained spectroscopic data of the shortened filaggrin peptide **4** is consistent with those of **3** within the macrocycle, while a low dispersion is visible for the N- and C-terminal amino acids. This suggests that the disulfide macrocycle 4–17 of **3** forms a well-defined  $\beta$ -hairpin, too, while the N-terminal amino acids 1–3 and the C-terminal 15–22 show no preferred conformation. The chemical shifts of the amino acids identical with **2**—Cys<sup>4</sup>, His<sup>5</sup>, Trp<sup>6</sup> and Leu<sup>15</sup>, Val<sup>16</sup>, Cys<sup>17</sup>—and the side-chain rotamers correspond to the data published by Cochran. Therefore the conformation of the  $\text{CX}_8\text{C}$  hairpin **2** is found in the  $\text{CX}_{12}\text{C}$  hairpin **3** and the folding of the model peptide is transferable to larger macrocycles.

Next, we determined whether the filaggrin peptide **3** has biological activity in spite of the mutations necessary for the stable folding. A dot blot assay was developed to analyze the

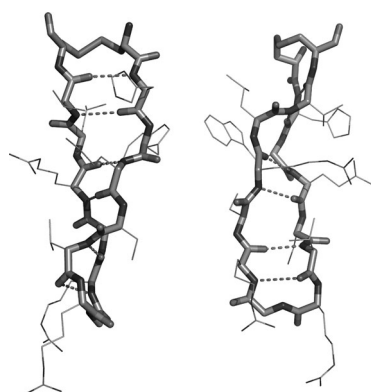


**Figure 5.** Two views of the structure model of the twisted  $\beta$ -hairpin structure of **4** based on NOE contacts between the peptide backbone and side-chain protons. The hydrogen bonds between the peptide backbone are represented by dashed lines. Val<sup>16</sup>/His<sup>5</sup> and Leu<sup>13</sup>/Trp<sup>6</sup> side chains are oriented toward each other. The citrulline side chain in the turn is twisted away from the peptide backbone and stands out from the whole peptide.

antibody recognition. The chimeric filaggrin peptide **3** and cfc1-cyc **1** were coated on a nitrocellulose membrane and incubated with biotin conjugated ACPA ( $\alpha$ -CCP, polyclonal, rabbit). The antibody binding was detected with HRP-conjugated streptavidin (Table 3). It was found that the mutant peptide **3** has a comparable affinity to **1**. Accordingly, the  $\beta$ -hairpin conformation of **3** has no negative influence on the binding affinity. This finding confirms the hypothesis that citrullinated peptides form a  $\beta$ -turn-like loop structure when bound to ACPA.

**Table 3:** Binding of filaggrin peptides to ACPA in the dot blot assay. The ornithine peptide **13** was used as a negative control.

Peptide <sup>[a]</sup>	Binding to ACPA <sup>[b]</sup>
KHQCHQESTXGRSRLVCGRSGS ( <b>1</b> )	+++
KHQCHWESTXGRSRLVCGRSGS ( <b>3</b> )	+++
KHQCHWESTXaRSRLVCGRSGS ( <b>11</b> )	–
KHQCHQESTXaRSRGRSGRSGS ( <b>12</b> )	+
KHQCHWESTOGRSRLVCGRSGS ( <b>13</b> )	–
KHQCHWESTXGRSRLICGRSGS ( <b>14</b> )	++
KHQCHQESTXGSKGKCGRSGS ( <b>15</b> )	+
KHQAHCESTXGRSRLCGRSGS ( <b>16</b> )	++

[a] Sequence of cyclic disulfide peptides. X = citrulline. [b] The number of plusses describes the intensity of the dot blot signal.

The dot blots of the peptides are shown in the Supporting Information. Remarkable are the results of the D-Ala<sup>11</sup> mutant of **3** (**11**) and of the D-Ala<sup>11</sup> mutant of **1** (**12**). As previously described, peptide **11** showed  $\beta$ -hairpin folding while **12** formed no preferred conformation. Both peptides showed a lower binding to ACPA than **1** and **3**, regardless of their structure. This suggests that not only the urea group of citrulline is essential for antibody recognition, but that the two amino acids Cit-Gly are bound by the antibody as the terminal loop of a  $\beta$ -hairpin. Apparently, the local stabilization of the turn structure with a D-amino acid leads to a decrease of the binding affinity. The induced  $\beta$ II'-turn has an

unfavorable rigid geometry for the antibody binding while the Cit-Gly turn can assume the optimal conformation for binding by a fast equilibrium between  $\beta$ I' and  $\beta$ II'.

A preselection of peptides was made from the dot blots. Selected peptides were subsequently tested against human ACPA in an ELISA for quantification of their antibody binding. Peptides were covalently linked to 96-well plates and incubated with ACPA ( $\alpha$ -CCP, polyclonal, human). Antibody binding was detected with HRP-conjugated anti human IgG antibody (Figure 6). Peptides **1** and **3** show a comparable binding to the human antibody, whereas the D-Ala<sup>11</sup> mutant of **1** (**12**) and the Orn<sup>10</sup> mutant of **3** (**13**) are hardly detected by ACPA. The different recognition of the D-Ala<sup>11</sup> mutant of **3** (**11**) by the different antibodies may be explained by the local stabilization of the  $\beta$ -turn. This will be shown by experiments with further peptides.

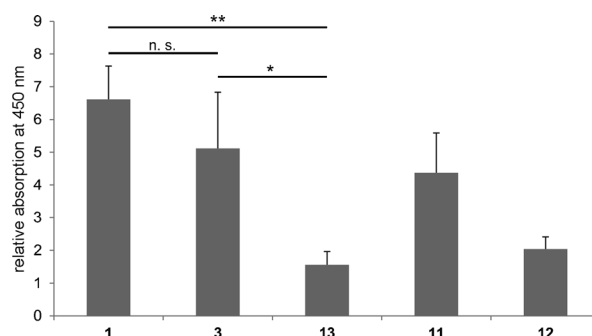


**Figure 6.** ELISA with ACPA (human). The relative absorption at 450 nm from three independent experiments is normalized to background absorbance. No significant difference could be detected between the absorption of the peptides **1** and **3**, while both are significantly higher than the negative control **13** (Student's *t* test:  $P > 0.05$  (n.s. (not significant)),  $P < 0.05$  (\*) or  $P < 0.01$  (\*\*)).

Conformational analysis by NMR spectroscopy and the study of biological activity demonstrated that it is possible to create chimeric peptides that combine the properties of two very different peptides. The structural motif of a cyclic  $\beta$ -hairpin peptide was integrated in the filaggrin sequence **1** by the mutation of three amino acids without adversely affecting its binding affinity. The transfer of stabilizing interactions from one peptide to another with different sequence and length provides important information about the folding properties of disulfide-bridged cyclic peptides. Apparently the motif CHWX<sub>n</sub>LVC ( $n = 4, 6, 8$ ) leads to hairpin conformation. It was shown that Val has a minor influence on folding, whereas Leu at this position is essential for the formation of the  $\beta$ -hairpin structure. Therefore, the stabilizing effects identified by Cochran for peptide **2** apply not only to the CX<sub>8</sub>C peptides, but are transferable to larger peptides, as shown for the CX<sub>12</sub>C motif in this work. The folding motif identified in the model peptide **2** can be integrated into a biologically active sequence. The measured data support the hypothesis that the filaggrin peptide **1** assumes a  $\beta$ -hairpin-type structure in the antibody binding pocket of ACPA, since the predetermined structure of **3** does not result in reduced binding affinity. Further structural constrictions will be



integrated in future generations of peptides to obtain more information about the solution structure and in the antibody-bound conformation. Preliminary experiments to obtain structured peptides without disulfides were unsuccessful as evident from the low signal dispersion.

The investigations of folded chimeric filaggrin peptides can provide important information about the nature of the peptide–antibody binding. In addition, it should be possible to filter polyclonal autoantibodies from mixtures of varying binding selectivities. This will assist the development of new specific ELISA test systems for a better early diagnosis of RA.

## Experimental Section

Peptides were synthesized on a peptide synthesizer with Fmoc strategy under standard conditions (3 equiv Fmoc amino acid, HBTU, HOBT, 8 equiv DIPEA, 2 × 1 h). For disulfide oxidation, peptides were dissolved in  $\text{NH}_4\text{HCO}_3$  buffer (10 mM, pH 7.4) and stirred in an open flask. Dot Blots were made on a nitrocellulose membrane. Peptides were applied to the membrane in different concentrations; free binding positions were blocked with Roti-Block. After incubating with biotin-conjugated ACPA ( $\alpha$ -CCP, rabbit, 2  $\mu\text{g mL}^{-1}$  in Roti-Block) for 1 h and with HRP-conjugated streptavidin (1  $\mu\text{g mL}^{-1}$  in Roti-Block) for 1 h, antibody binding was detected with ECL substrate on a photographic film. ELISAs were made in 96-well plates (DNA-Bind Surface, Corning). Peptides were dissolved in  $\text{NaHCO}_3$  buffer (50 mM, pH 9.6) and 0.5  $\mu\text{g/well}$  was added. Plates were blocked overnight with 2% BSA in  $\text{NaHCO}_3$  buffer and incubated with ACPA ( $\alpha$ -CCP, human, in PBS-T) for 1 h. After incubating the plates with HRP-conjugated anti human IgG (0.3  $\mu\text{g mL}^{-1}$  in PBS-T) for 30 min TMB solution and 5%  $\text{H}_2\text{SO}_4$  were added and the color reaction detected at 450 nm.

Received: November 13, 2013

Revised: January 15, 2014

Published online: March 5, 2014

**Keywords:** disulfides · filaggrin · NMR spectroscopy · peptides ·  $\beta$ -hairpin

- [1] G. A. Schellekens, B. A. de Jong, F. H. J. van den Hoogen, L. B. van de Putte, W. J. van Venrooij, *J. Clin. Invest.* **1998**, *101*, 273–281.

- [2] E. Girbal-Neuhausser, J.-J. Durieux, M. Arnaud, P. Dalbon, M. Sebbag, C. Vincent, M. Simon, T. Senshu, C. Masson-Bessiere, C. Jolivet-Reynaud, et al., *J. Immunol.* **1999**, *162*, 585–594.
- [3] G. A. Schellekens, H. Visser, B. A. de Jong, F. H. J. van den Hoogen, J. M. Hazes, F. C. Breedveld, W. J. van Venrooij, *Arthritis Rheum.* **2000**, *43*, 155–163.
- [4] M. A. M. van Boekel, E. R. Vossenaar, F. H. J. van den Hoogen, W. J. van Venrooij, *Arthritis Res.* **2002**, *4*, 87–93.
- [5] N. Bizzaro, G. Mazzanti, E. Tonutti, D. Villalta, R. Tozzoli, *Clin. Chem.* **2001**, *47*, 1089–1093.
- [6] K. Suzuki, T. Sawada, A. Murakami, T. Matsui, S. Tohma, K. Nakazono, M. Takemura, Y. Takasaki, T. Mimori, K. Yamamoto, *Scand. J. Rheumatol.* **2003**, *32*, 197–204.
- [7] W. J. van Venrooij, J. M. Hazes, H. Visser, *Neth. J. Med.* **2002**, *60*, 383–388.
- [8] W. J. van Venrooij, J. J. B. C. van Beers, G. J. M. Pruijn, *Ann. N. Y. Acad. Sci.* **2008**, *1143*, 268–285.
- [9] A. S. Wiik, W. J. van Venrooij, G. J. M. Pruijn, *Autoimmun. Rev.* **2010**, *10*, 90–93.
- [10] T. Pérez, A. Gómez, R. Sanmarti, O. Viñas, G. Ercilla, I. Haro, *Lett. Pept. Sci.* **2002**, *9*, 291–300.
- [11] H. Jane, P. E. Wright, *FASEB J.* **1995**, *9*, 37–42.
- [12] S. Pandey, M. C. Alcaro, M. Scrima, E. Peroni, I. Paolini, S. Di Marino, F. Barbetti, A. Carotenuto, E. Novellino, A. M. Papini, et al., *J. Med. Chem.* **2012**, *55*, 10437–10447.
- [13] F. Lolli, B. Mulinacci, A. Carotenuto, B. Bonetti, G. Sabatino, B. Mazzanti, A. M. D'Ursi, E. Novellino, M. Pazzagli, L. Lovato, et al., *Proc. Natl. Acad. Sci. USA* **2005**, *102*, 10273–10278.
- [14] J. Brown, R. Teller, *J. Am. Chem. Soc.* **1976**, *98*, 7565–7569.
- [15] R. Haubner, R. Gratias, B. Diefenbach, S. L. Goodman, A. Jonczyk, H. Kessler, *J. Am. Chem. Soc.* **1996**, *118*, 7461–7472.
- [16] R. Haubner, D. Finsinger, H. Kessler, *Angew. Chem.* **1997**, *109*, 1440–1456; *Angew. Chem. Int. Ed. Engl.* **1997**, *36*, 1374–1389.
- [17] K. Moehle, Z. Athanassiou, K. Patora, A. Davidson, G. Varani, J. A. Robinson, *Angew. Chem.* **2007**, *119*, 9260–9264; *Angew. Chem. Int. Ed.* **2007**, *46*, 9101–9104.
- [18] B. Eckhardt, W. Grosse, L.-O. Essen, A. Geyer, *Proc. Natl. Acad. Sci. USA* **2010**, *107*, 18336–18341.
- [19] S. J. Russell, T. Blandl, N. J. Skelton, A. G. Cochran, *J. Am. Chem. Soc.* **2003**, *125*, 388–395.
- [20] A. G. Cochran, R. T. Tong, M. A. Starovasnik, E. J. Park, R. S. McDowell, J. E. Theaker, N. J. Skelton, *J. Am. Chem. Soc.* **2001**, *123*, 625–632.
- [21] H. Kessler, *Angew. Chem.* **1982**, *94*, 509–520; *Angew. Chem. Int. Ed. Engl.* **1982**, *21*, 512–523.
- [22] HyperChem, Hypercube, Inc., Gainesville, FL, **2000**.